# DEVELOPMENT AND CHARACTERIZATION OF SURFACE MICRO-MACHINED MEMS BASED VARACTOR

*Subha Chakraborty[1], A. Bhattacharya[1], Ashesh Ray Chaudhuri[2] and T.K. Bhattacharyya[1]

Dept. of Electronics and Electrical Communication Engineering[1], Advanced Technology Development Centre[2]

Indian Institute of Technology Kharagpur

Kharagpur – 721302, India.

*Email: subharpe@gmail.com

***Abstract- This paper presents complete behavioral analysis of a surface micro-machined MEMS varactor for frequency tuning application in voltage controlled oscillators in RF applications with high Quality factor and tunability. The dimensions of the MEMS device have been optimized with Finite Element Method based CoventorWare analysis and verified through lumped parameter analysis in Saber platform. The MEMS varactor has been fabricated with the PolyMUMPs process. The paper also describes the Mechanical and electrical characterization of the MEMS varactor to meet the designed specification.***

**Index terms*: MEMS, varactor, VCO, capacitance tuning ratio, pull-in, SEM, vibration spectrum, LDV.***

## I. INTRODUCTION

Most of the Modern wireless communication systems demand voltage controlled oscillators (VCOs) with wide tuning range, low power, low phase noise and high quality factor in the giga-hertz frequency range of operation [1]-[2]. The tuning range should be wide enough to cover the entire frequency band. LC tuned VCO is normally used in different blocks of a wireless transceiver such as a frequency synthesizer or a PLL due to its better phase noise performance in comparison to a ring oscillator. The tunability of a VCO is normally provided by the varactor present at the tank circuit of the VCO. Lesson's formula of phase noise of a VCO describes the inverse square relationship between phase noise and Q factor of the tank circuit [3]. From that, it is evident that phase noise performance can be improved by increasing the Q factor of the tank

circuit. Since on-chip inductors do not possess very high Q values, Q factor of the varactor device needs to be increased.

It is difficult to realize on-chip variable capacitor that has low phase noise and high quality factor and can work over wide process and temperature variation [1]. MEMS Based varactors are a very good replacement of the on-chip MOS varactors in this regard. Due to low loss, MEMS varactors not only possess the property of very high Q values capable of withstanding wide process and temperature variation [4], but they do also exhibit more linearity and output voltage swing handling capability than the p-n junction varactors. Surface micro-machined electro-statically actuated parallel plate capacitor with quality factor as high as 60 at 1 GHz has been reported [1], [5]-[7]. MEMS based varactors that show capacitance variation less than 6% with wide temperature range have also been achieved [8].

This presented work describes development of a MEMS variable capacitor for VCO application using the method of electrostatic actuation. The operating principle is derived from varying the gap between the two parallel plates of the capacitor using electrostatic actuation, one of which is fixed and other one held suspended for movement under electrostatic force of attraction due to the actuation voltage.

Optimization of the capacitor dimensions have been achieved using *CoventorWare* [9] simulation. The electro-mechanical lumped parameter representation of the same has been realized in *Saber* platform. The device has been fabricated with *PolyMUMPs* [10] surface micromachining process. To validate the simulation results, mechanical and electrical testing have been performed using Laser Doppler Vibrometer (LDV) and Wafer prober with LCR meter setup respectively.

## II. WORKING PRINCIPLE OF VARACTOR

The varactor structure is a surface micromachined quad beam structure. It has a conducting electrode underneath the proof-mass with air gap in between. When a dc potential is applied to the electrode with the proof-mass grounded, due to electrostatic actuation, the air gap reduces; resulting in an increase in the parallel plate capacitance. Thus, by changing the applied potential, the structure can be made to operate as a variable capacitor [11].

The value of the capacitance between the two plates can be written as [12]

$$C = \frac{\varepsilon_0 A}{(x_0 - x)} \tag{1}$$

where $\varepsilon_0$ is the permittivity of free space, $A$ is the overlapping area between the two parallel plates, $x_0$ is the initial gap between the two plates and $x$ is the deflection due to the applied actuation voltage.

Considering a spring-mass model of the varactor structure as shown in fig. 1, the steady deflection of the moving plate due to an applied voltage $V$ is found using the balance between the electrostatic force and the restoring elastic force in the deflected beam [13]

$$\frac{\varepsilon_0 W w V^2}{(x_0 - x)^2} = kx \tag{2}$$

where $W$ and $w$ are the length and breadth of the plates and $k$ is spring constant.

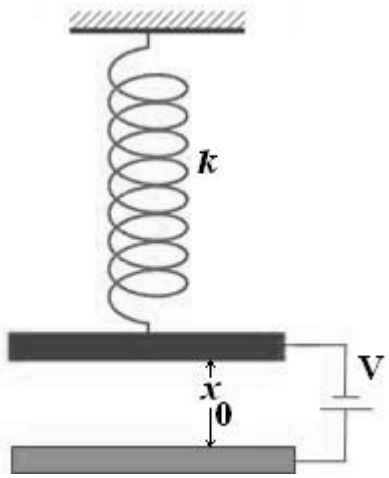


Figure 1. Spring-mass model of the varactor structure

It can be shown by solving equation (2) that if the applied voltage is limited within a critical value, called the *pull-in voltage*, the deflection of the moving plate is also limited to steady values within $x_0/3$, and if the voltage exceeds the pull-in limit, the moving plate crashes on the bottom plate [13]. The pull-in voltage is given by

$$V_p = \sqrt{\frac{8kx_0^3}{27W w \varepsilon_0}} \tag{3}$$

Therefore if the applied voltage is ensured not to exceed $V_p$, steady gap modulation between the plates and hence change in capacitance is achievable.

Ideally, the tuning range of this design is 1.5:1 and is limited by the pull-in effect. This is due to the fact that

$$TR = \frac{C_{\max}}{C_{\min}} = \frac{\varepsilon A/(2x_0/3)}{\varepsilon A/(x_0)} = 1.5 \tag{4}$$

Incorporating a worst-case-scenario fringing capacitance $C_f$ of 40% of $C_{max}$ as indicated in [13], the value of capacitance tuning ratio is obtained as follows [14]

$$TR = \frac{C_{\max} + C_f}{C_{\min} + C_f} = \frac{C_{\max} + 0.4C_{\max}}{C_{\min} + 0.4C_{\max}} = 1.3125 \tag{5}$$

since $C_{max} = 1.5C_{min}$.

## III. DESIGN AND SIMULATION OF VARACTOR

The varactor structure, as shown in fig. 2, consists of a centrally placed rectangular polysilicon proof-mass which is suspended with four symmetrically placed polysilicon beams; two are on one side and two on other. All these beams are rigidly clamped from two fixed walls on each side. Also, there is a polysilicon electrode placed underneath the proof-mass; with air gap in between. The dimensions of the structure are given in Table I [15].

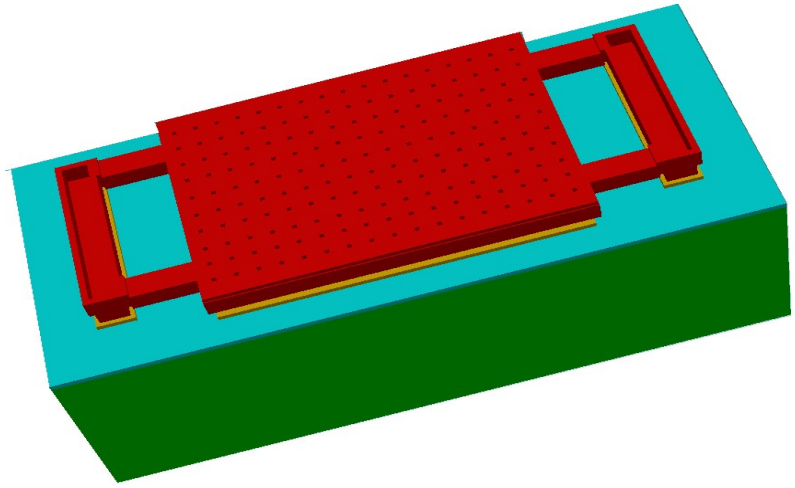

Figure 2. 3-D view of the MEMS varactor

Table1. Design parameters of the MEMS varactor

| | |
|---|---|
| Silicon substrate | $648\mu m \times 288\mu m \times 20\mu m$ |
| Nitride | $648\mu m \times 288\mu m \times 0.6\mu m$ |
| Actuation electrode | $320\mu m \times 220\ \mu m \times 0.5\mu m$ |
| Proof-mass | $350\mu m \times 250\mu m \times 2\ \mu m$ |
| Beam | $100\mu m \times 20\ \mu m \times 2\ \mu m$ |
| No. of beams | *4* |

To realize the MEMS varactor model in *Saber* software, parallel conductor plates and clamped beams have been clubbed together and assigned with a particular point as knot in the 3-dimensional space as shown in fig. 3.

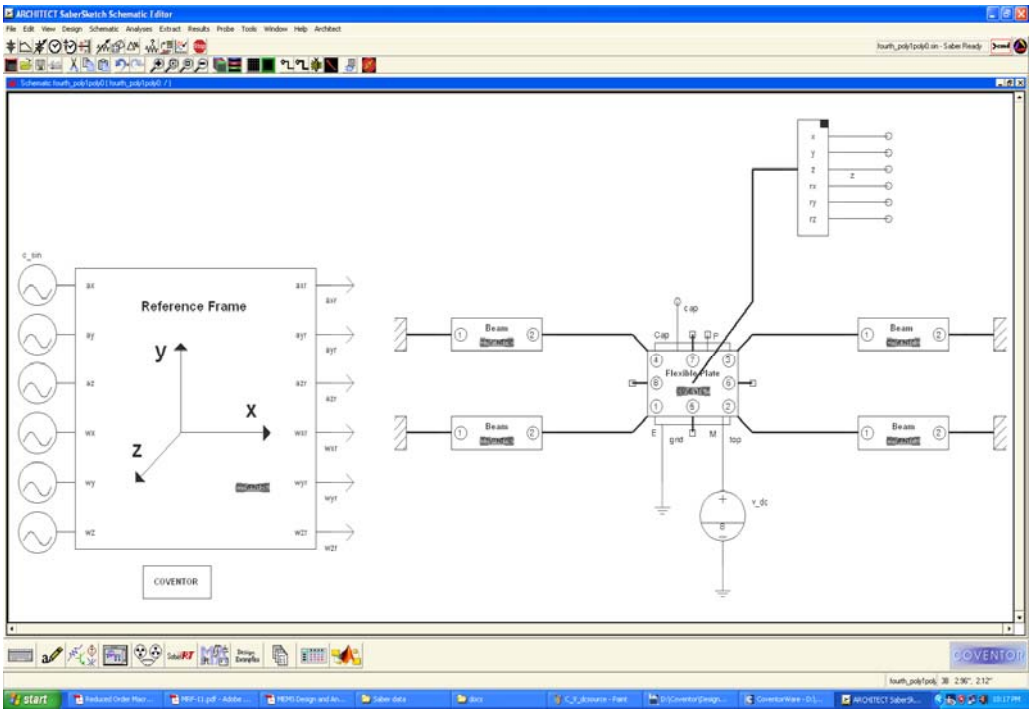


Figure 3. System model of the quad-beam varactor in *Saber*

Small signal frequency analysis of the structure has been done in *Saber*. The simulated vibration spectrum showing the first three harmonics at 36.096 kHz, 188.68 kHz and 457.47 kHz is given in fig. 4. The corresponding mode shapes at the three modes of vibration is shown in figures 5, 6 and 7 respectively.

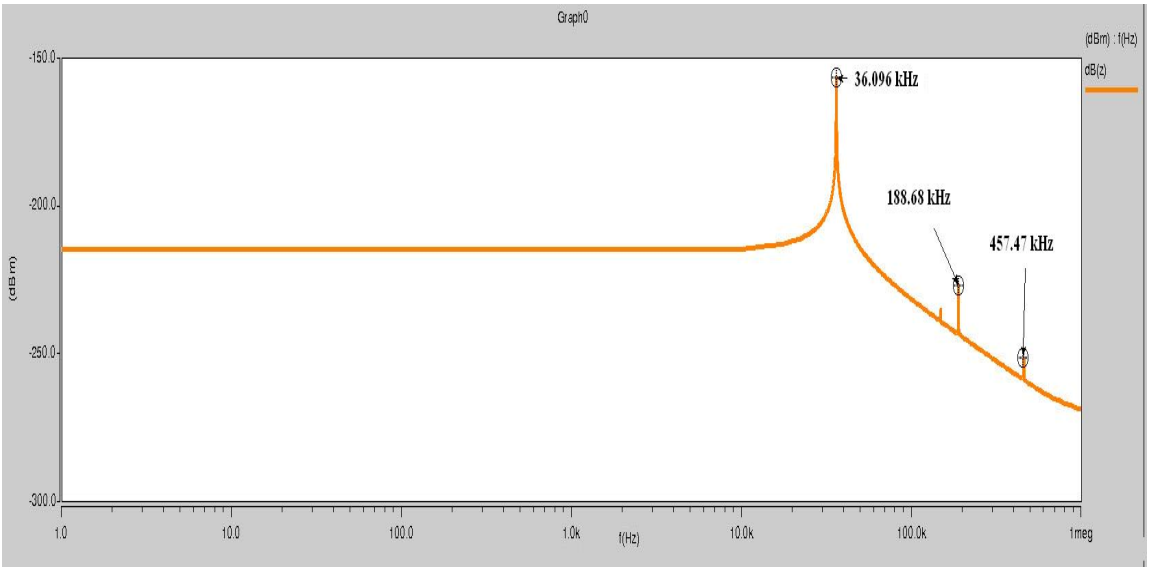


Figure 4. Simulated vibration spectrum of the varactor

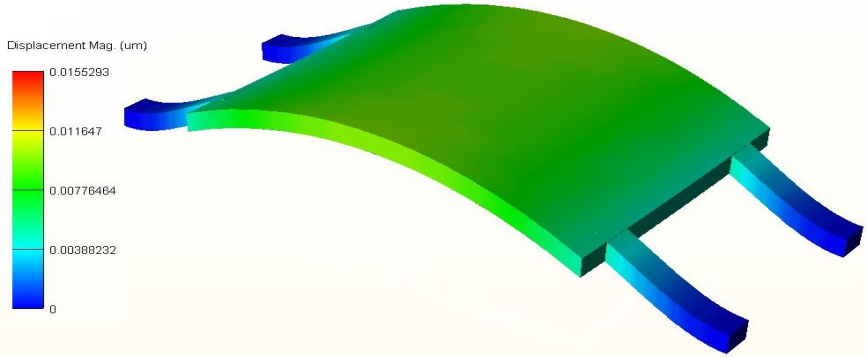


Figure 5. First mode of vibration

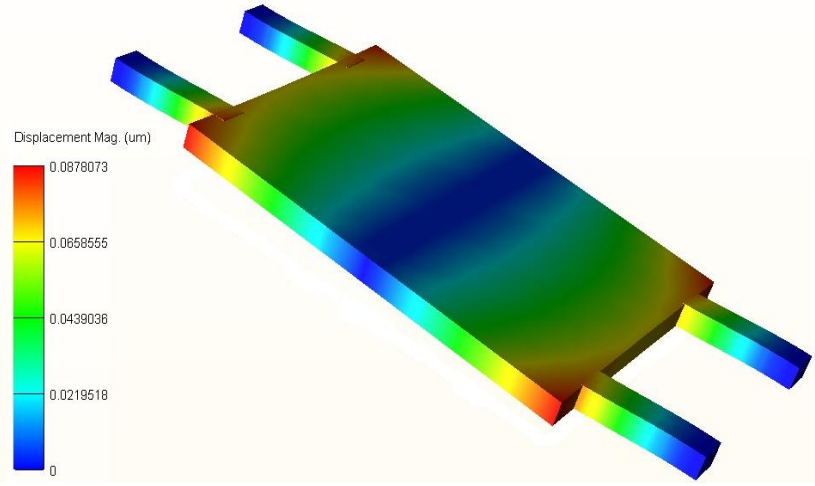


Figure 6. Second mode of vibration

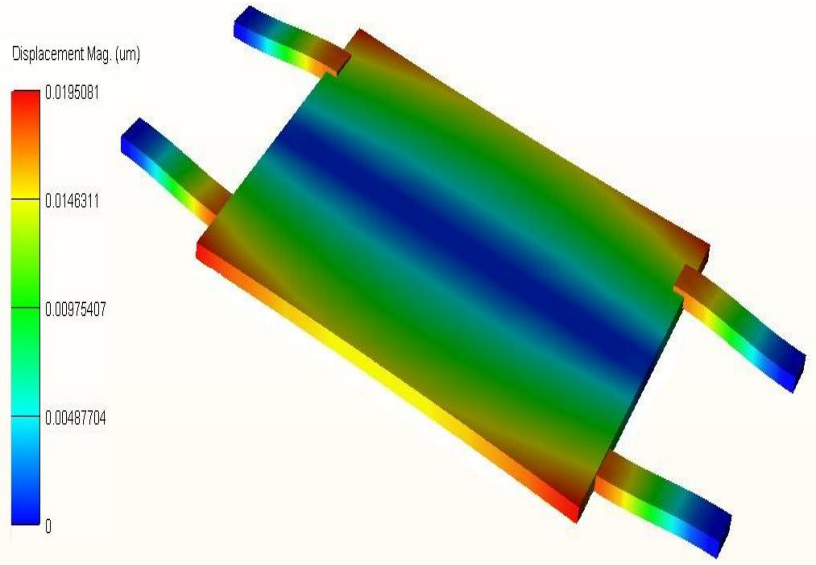


Figure 7. Third mode of vibration

The pull-in voltage is simulated in *Saber* using "*Arc Length Continuation Voltage with Position Input*" model which overcomes the typical convergence discontinuities during pull-in by moving along the force balance curve. The variation of beam deflection with the actuation voltage for the structure, obtained from *Saber Architect* simulation is presented in the fig. 8. A semi-analytical model of the pull-in voltage can be obtained from [16] which calculated the total potential energy content of a fixed-fixed beam subjected to electrostatic without considering the fringing field effects, and then a correction factor is applied to account for the fringing field effects. The first-order fringing field effects have been approximately compensated by an effective beam width. Following [16], the pull-in voltage can be calculated from:

$$V_P = \sqrt{\frac{1}{\left(1+0.65\frac{x_0}{w}\right)}} \times \sqrt{\frac{c_1 E h^3 {x_0}^3}{\varepsilon_0 l^4} + c_2 \frac{(1-\nu) x_0 h \sigma_0}{\varepsilon_0 l^2}} \tag{6}$$

where the constants $c_1$=11.7 and $c_2$=3.6, $E$ is the Young's modulus and $\nu$ is the Poisson's ratio, $x_0$ is the gap between the two parallel plate, $l$ and $h$ is the beam length and width respectively, $w$ is the thickness of the beam and $\varepsilon_0$ is the permittivity of free space.

From fig. 8, we find the pull-in voltage of the device is about 8.81 volts.

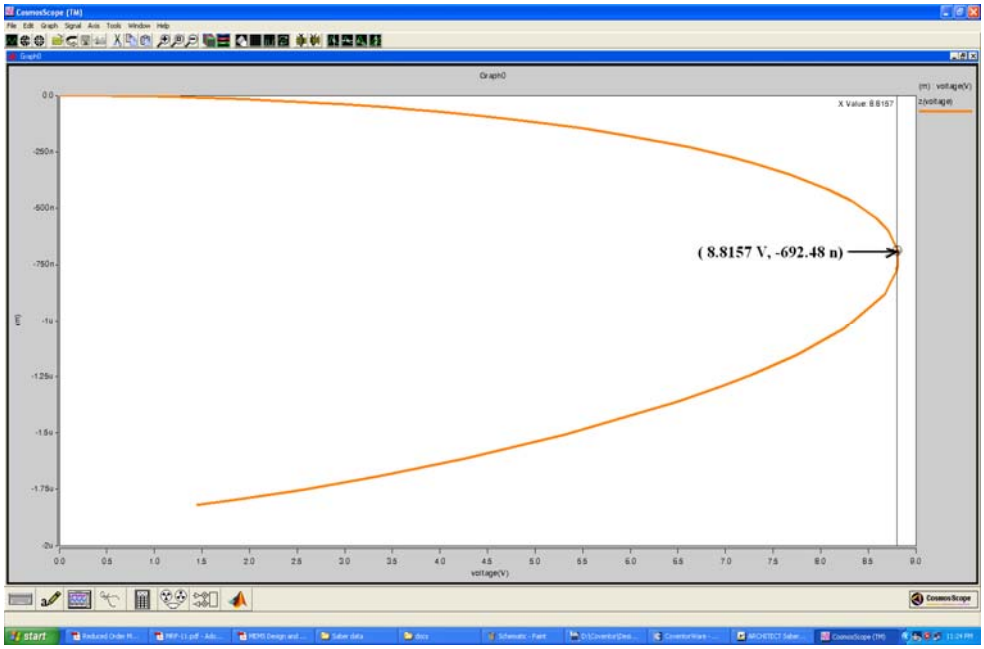


Figure 8. Variation of deflection with applied voltage for pull-in detection

To determine the voltage versus capacitance characteristics of the particular device, we applied a voltage sweep between the two plates of the varactor and the simulated C-V characteristic is as shown in fig. 9. From the plot we find that the maximum capacitance available from the device is about 574.29fF and the minimum value around 387.37fF. The capacitance ratio for the device is therefore about 1.48:1.

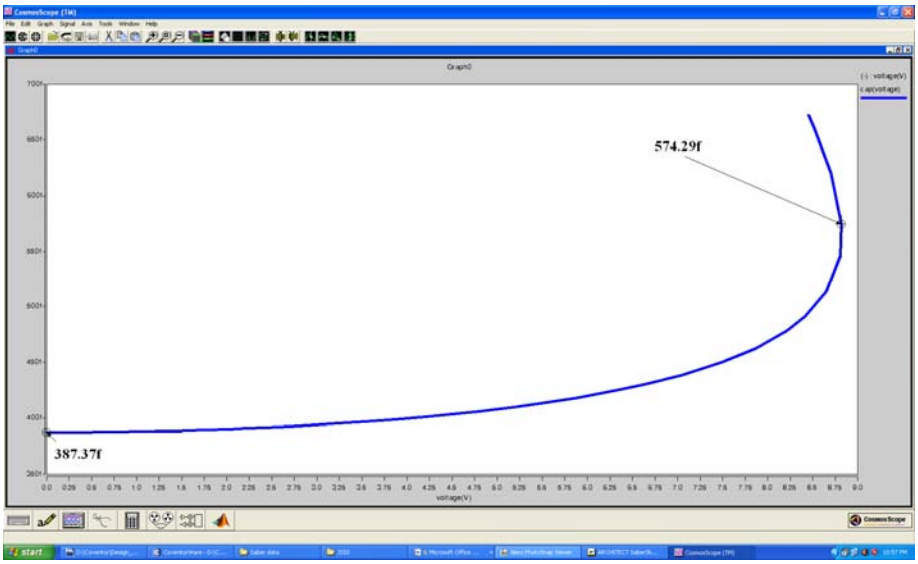


Figure 9. Capacitance variation with actuation voltage

## IV. FABRICATION OF VARACTOR STRUCTURE

The structure has been fabricated using standard *PolyMUMPs* surface micro-machining process. The layout of the varactor, designed in L-Edit [17] (Tanner tool) is shown in fig. 10. Silicon wafer is used as the substrate material and Silicon Nitride as an insulating layer on top of the substrate. *PolyMUMPs* is a surface micro-machined CMOS compatible process where all the electrical connections are taken from the first conformal polysilicon layer named as *Poly0*, the bottom plate of the varactor is also realized using the same *Poly0* layer. This bottom plate is fixed on the substrate; the other flexible plate of the varactor is realized with the *Poly1* layer. The *Poly1* layer has been selectively etched using the Deep Reactive Ion Etching (DRIE) process to realize the quad-beam proof mass structure and it is fixed to the substrate employing the Anchor process. The electrical connection from the *Poly1* layer is breached through the anchors to *Poly0* layer. Perforations are added to the *Poly1* layer using the *Hole1* masking layer to help in releasing the proof-mass structure from stiction. These also help to reduce the squeezed film air damping in the gap between proof-mass and electrode. The SEM image of the fabricated structure has been shown in Fig. 11.

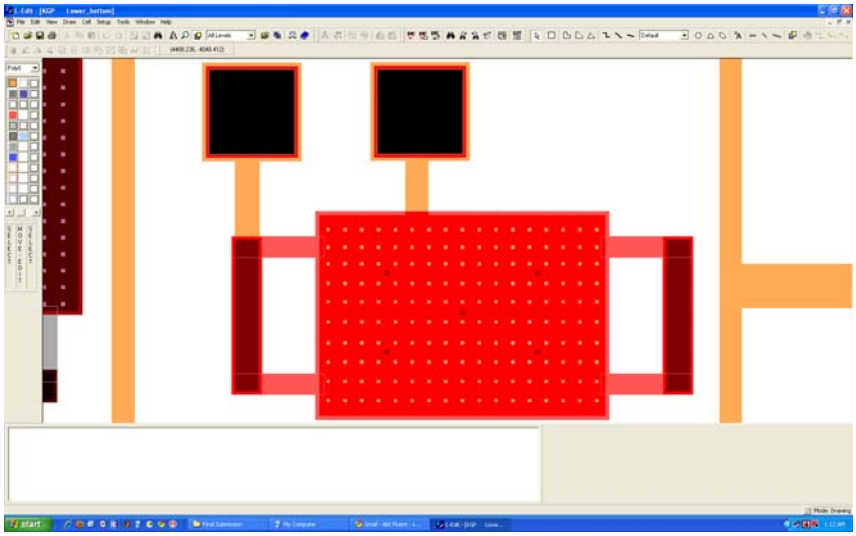

Figure 10. Layout of the quad-beam varactor structure

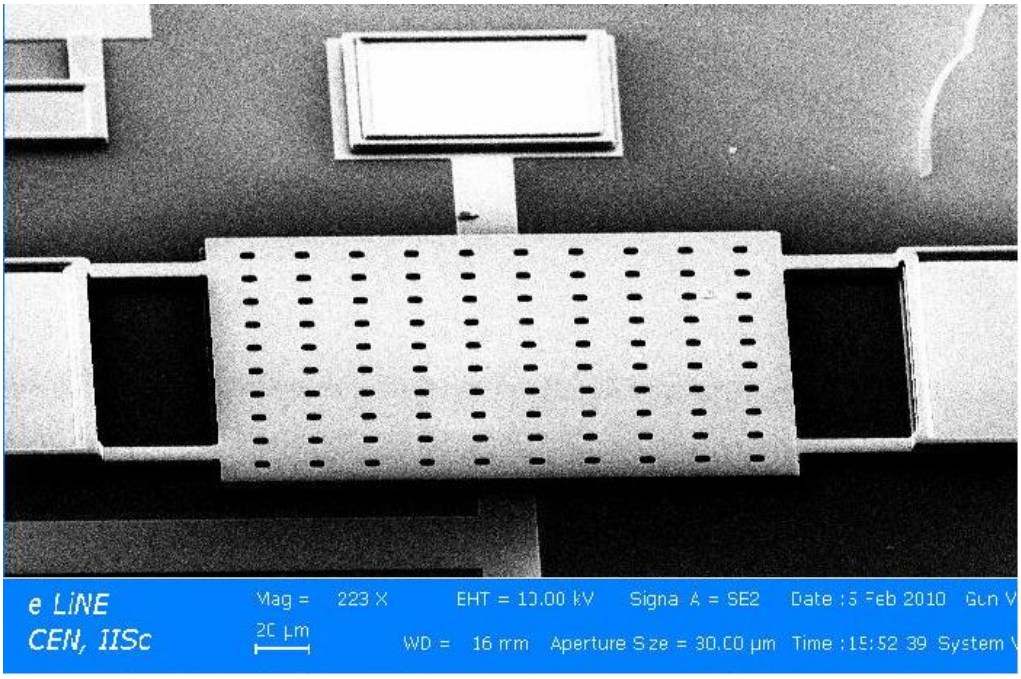


Figure 11. SEM image of the fabricated varactor structure

## V. TESTING AND CHARACTERIZATION OF VARACTOR

The Mechanical and electrical tests has been performed on the varactor to examine the characteristics of the structure. Voltage actuation method has been used to detect the mechanical vibrations of the varactor. Small signal frequency sweep has been imposed over a dc actuation voltage to observe the frequency response of the particular structure. The out-of-plane vibration amplitude response has been recorded for the frequencies of the signal. Polytec made Laser Doppler Vibrometer (LDV) has been used to detect the displacement of the structure in the out of plane direction. The LDV uses Doppler frequency shift method to calculate displacement due to external excitation at the point on the where the laser pointer is focused. The vibration spectrum of the MEMS varactor with applied external excitation has been shown in fig 12. The first mode of vibration of the structure at 27.5 kHz which is obtained from LDV is given in fig. 13.

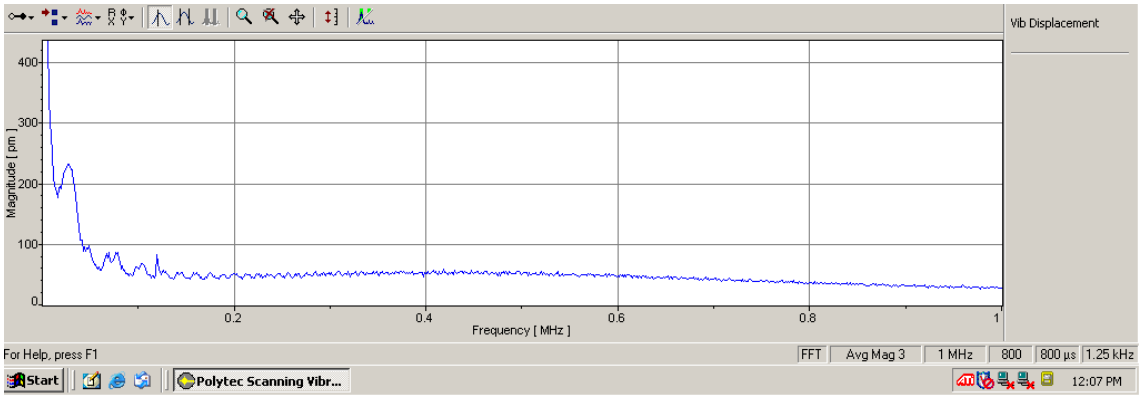


Figure 12. Vibration spectrum of the MEMS varactor

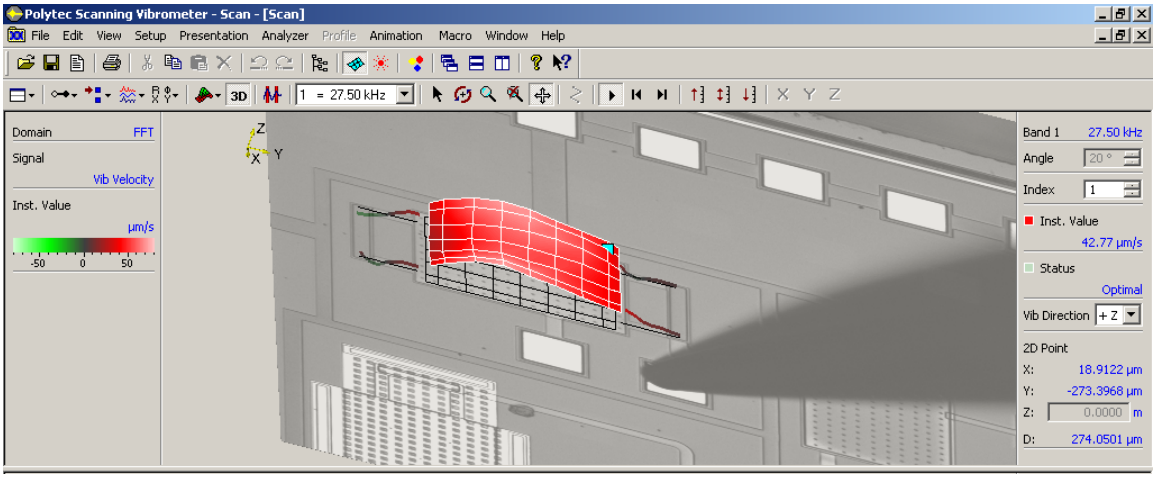


Figure 13. First mode of vibration

The variation of capacitance with actuation voltage of the structure has been performed using a DC probe station manufactured by Sus-Microtec, DC voltage source and a LCR meter manufactured by Agilent. To measure the C-V characteristics, the bottom fixed plate of the varactor has been grounded and the required voltage sweep from 0 volt to 9 volt has been applied to the top suspended electrode using the probes. A small AC signal of 5MHz has been imposed on the DC actuation voltage to measure the capacitance. Open circuit offset measurement corrections were made before recording the capacitance values. The capacitance of the varactor with change in voltage has been observed and plotted by the LCR meter as shown in fig. 14.

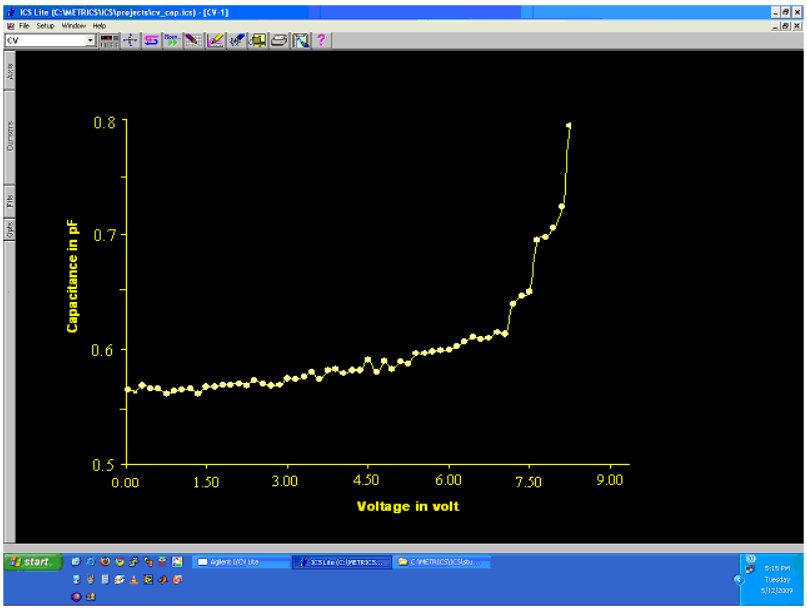


Figure 14. Measured capacitance variation with applied voltage

From the measured capacitances, the maximum and minimum capacitances available from the device are 0.80pF and 0.56pF respectively.

## VI. DISCUSSIONS

This paper presents the development of a MEMS varactor including design, simulation, fabrication process and functional testing. A comparison between the simulated and tested results is mentioned below.

The fundamental mode of vibration from LDV measurements is found within 24% tolerance from the simulation result as mentioned in Fig. 4. The variation in the value is quite acceptable as test condition includes unavoidable environmental perturbations, damping and process variations which are not considered in the simulation. Also, the variation of capacitance with actuation voltage as obtained from testing and depicted in fig. 14 shows that the capacitance tuning ratio of the Varactor is about 1.43:1 which greatly conforms to the simulation values. The sudden change in the measured capacitance at around 8.2 volts manifests the pull-in condition.

## ACKNOWLEDGEMENT

We would like to acknowledge Prof. Rudra Pratap and Prof. Navakanta Bhatt and the group-members for their support and help in performing the tests at IISc, Bangalore. We also thank National Programme on Micro and Smart Systems (NPMASS) for sponsoring projects on MEMS based varactors at Advanced Technology Development Centre, IIT Kharagpur.

## REFERENCES

[1] Aleksander Dec and Ken Suyama, “Microwave MEMS-Based Voltage-Controlled Oscillators”, IEEE Transaction On Microwave Theory And Techniques, vol. 48, no. 11, pp. 1943-1949, Nov 2000.

[2] Aleksander Dec and Ken Suyama, “Micromachined Electro-Mechanically Tunable Capacitors and Their Applications to RF IC’s ”, IEEE Transaction On Microwave Theory And Techniques, vol. 46, no. 12, pp. 2587-2596, Dec. 1998.

[3] Thomas H. Lee and Ali Hajimiri, “Oscillator Phase Noise: A Tutorial”, IEEE Journal of Solid State Circuits, vol. 35, no. 3, pp. 326-336, March 2000.

[4] A Ray Chaudhuri, S. Chakraborty, A Bhattacharya, R. Ray Chaudhuri and T. K. Bhattacharyya, “System Level Realization and Analysis of MEMS Integrated Voltage Controlled Oscillator”, IEEE Applied Electromagnetics Conference (AEMC 09), Dec. 2009.

[5] Young, D. and Boser, B., “A micromachined variable capacitor for monolithic low-noise VCOs.”, IEEE Solid State Sensor and Actuator Conference, pp 86-89, 1996.

[6] Prabir K. Saha, Ashudeb Dutta, Tarun K. Bhattacharyya and Amit Patra, “Effects of active Q enhancement on oscillator phase noise: an analysis”, Analog Integrated Circuits and Signal Processing, vol. 52, Issue 3, pp: 99 – 107, September 2007.

[7] A Dec and Ken Suyama, “RF micromachined varactor with wide tuning range”, IEEE RFIC symp. Dig 1, pp 309-312, June 1998.

[8] Nieminen H., Ermolov V., Silanto S., Nybergh K. and Ryhanen, T., "Design of a temperature-stable RF MEM capacitor", IEEE journal of Microelectromechanical System, vol. 13, Issue 5, pp: 705–714, Oct. 2004.

[9] "MEMS Design and Analysis Tutorials, Vol. 1, Physical and System-Level Design," CoventorWare, Version 2008.

[10] PolyMUMPs Design Handbook, Revision 11.0.

[11] A Bhattacharya, R. Ray Chaudhuri, A. Ray Chaudhuri, S. Chakraborty and T.K. Bhattacharyya, "Reduced Order Macromodel Extraction of MEMS Based Varactor and Its System Level Simulation for RF Applications", 4th International Conference on Computers and Devices for Communication (CODEC 09), pp. 1-4, Dec. 2009.

[12] Michael S. McCorquodale, Mei Kim Ding and Richard B. Brown, "A CMOS Voltage-to-Frequency Linearizing Preprocessor for Paralie1 Plate RF MEMS varactors", IEEE Radio Frequency Integrated Circuits Symposium, pp 535-538.

[13] Gabriel M. Rebeiz, RF MEMS: Theory, Design and Technology, Wiley, 2003, pp 36–38.

[14] Amro M. Elshurafa and Ezz I. El-Masry, "Design Considerations in MEMS Parallel Plate Capacitors", 50th Midwest Symposium on Circuits and Systems, 2007(MWSCAS 2007), pp. 1173-1176, 2007.

[15] Anirban Bhattacharya, Ritesh Ray Chaudhuri, Ashesh Ray Chaudhuri, Subha Chakraborty and T.K. Bhattacharyya, "Squeezed-Film Damping Performance Comparison of Perforated and Non-perforated Surface Micromachined Quad-beam Structures", Third National Conference on MEMS, Smart Structures and Materials (ISSS – 2009), pp. 118-121, Oct, 2009.

[16] C. O'Mahony, M. Hill, R. Duane, and A. Mathewson, "Analysis of Electromechanical Boundary Effects on the Pull-in of Micro-machined Fixed–Fixed Beams", Journal of Micromechanics and Microengineering, Vol. 13, No. 4, pp. 75–80, Jul. 2003.

[17] L-Edit Win 32 8.30, www.tannereda.com.